Polymer 49 (2008) 3413–3418

Contents lists available at ScienceDirect

Polymer

journal homepage: www.elsevier.com/locate/polymer

The effect of synthesis procedure on the structure and properties of palladium/polycarbonate nanocomposites

O.P. Valmikanathan [a], O. Ostroverkhova [a], I.S. Mulla [b], K. Vijayamohanan [b], S.V. Atre [a,*]

[a] Oregon Nanoscience and Microtechnologies Institute, Oregon State University, Corvallis, OR 97331, United States
[b] Department of Physical and Materials Chemistry Division, National Chemical Laboratory, Pune 411008, India

ARTICLE INFO

Article history:
Received 27 January 2008
Received in revised form 19 May 2008
Accepted 21 May 2008
Available online 3 June 2008

Keywords:
Nanocomposites
In situ and *ex situ* syntheses
Morphology

ABSTRACT

In this paper, we compare two procedures for the synthesis of palladium (Pd)/polycarbonate (PC) nanocomposites as well as their morphological, optical, thermal and electrical properties. Pd nanoclusters were produced by the reduction of palladium chloride using a variation of Brust's method. Discrete Pd nanoclusters of ~15 nm size were formed in the absence of PC in the reaction mixture (*ex situ* method) while agglomeration of Pd nanoclusters was noticed in the presence of PC in the reaction mixture (*in situ* method). Fourier transform infrared spectroscopy (FTIR) suggests nanoparticle–polymer interactions and polymer conformational changes in the *in situ* nanocomposite films. Even after having the same Pd content, the *ex situ* nanocomposites films were found to transmit more light than the *in situ* nanocomposites. The glass transition temperature (T_g), decreased by ~16 °C for both the *ex situ* and *in situ* samples. Thermogravimetric analysis (TGA) indicated that the presence of Pd nanoclusters significantly improved the thermal stability of the nanocomposites, as evidenced by the enhanced onset of degradation by ~20 °C and ~40 °C for the *in situ* and *ex situ* nanocomposites, respectively. The electrical conductivity measurement shows a dramatic difference between these nanocomposites with a significantly higher value for the *in situ* nanocomposite (resistivity = 2.1×10^5 Ωm) compared to the *ex situ* nanocomposite (resistivity = 7.2×10^{13} Ωm).

1. Introduction

In the past few years, nanoclusters protected by polymers [1,2] and organic ligands [3–5] have gained increased attention in materials' research as they offer immense opportunities to design materials with tunable properties. For example, these nanoclusters have been shown to display variations in optical, thermal, electrical and electrochemical properties based on their size. Many of these properties were found to be controlled by the selection of the polymer as well as the distribution of the nanoclusters within the polymer matrix [6,7].

Generally, polymer-protected nanoclusters can be prepared by two different synthetic methods. In the *ex situ* method, organic ligand-protected nanoclusters are initially prepared followed by homogenous mixing with a polymer solution. In contrast, the *in situ* method, involves the preparation of nanoclusters in the presence of a polymer. This method generally involves no additional organic ligands as protecting agents other than the polymer. The resulting solutions from either method can subsequently be cast into films.

Several variants of the *ex situ* method have been reported for the preparation of metal/polymer nanocomposites. For example, dodecanethiol protected gold (Au) nanoclusters were added to styrene or methyl methacrylate monomer and subsequently polymerized [8]. Multilayer films were prepared from Au nanoclusters and chitosan solution [9]. Sputtering of Au nanoclusters on a polystyrene (PS) film has also been reported [10]. Variations of the *in situ* method have also been reported previously. For example, thermo-labile metallic precursors such as palladium acetate ($Pd(OAc)_2$) have been added to a solution of polymethyl methacrylate (PMMA) in toluene followed by thermolysis to form polymer-protected metallic nanoclusters [11]. Films have been obtained by reducing $Pd(OAc)_2$ in the presence of aniline followed by polymerization to form Pd/polyaniline nanocomposites [12]. Monophasic reduction of gold chloride ($HAuCl_4$) in the presence of PMMA was also used to produce polymer/metal nanocomposites [13].

From the earlier studies [14–23], it can be inferred that the morphology of the resulting nanoclusters depends on several factors such as molecular weight of the protecting agent; metal salt:protecting agent ratio; functional groups in the protecting agents; reaction temperature; reducing agent; and reduction rate. However, there have been few prior reports pertaining to directly

* Corresponding author. Oregon Nanoscience and Microtechnologies Institute, 106 Covell Hall, Oregon State University, Corvallis, OR 97331, United States. Tel.: +1 541 737 8272; fax: +1 541 737 5241.
E-mail address: sundar.atre@oregonstate.edu (S.V. Atre).

0032-3861/$ – see front matter © 2008 Elsevier Ltd. All rights reserved.
doi:10.1016/j.polymer.2008.05.036

exploring the effect of the *in situ* and *ex situ* nanocomposite synthesis methods on the structure and properties of the resulting metal/polymer nanocomposite films.

Here we report an *in situ* method for preparing nanocomposite films by reducing palladium chloride ($PdCl_2$) in the presence of polycarbonate (PC) dissolved in dichloromethane. We also synthesized Pd/PC nanocomposite films by an *ex situ* method involving the dispersion of dodecanethiol-protected Pd nanoclusters in a solution of PC in dichloromethane. These nanocomposite films were characterized by transmission electron microscopy (TEM), Fourier transform infrared spectroscopy (FTIR), UV–vis spectroscopy, thermal analysis [thermogravimetric analysis (TGA) and differential scanning calorimetry (DSC)] and electrical conductivity measurements. It was found that the synthesis method had a significant impact on the morphological characteristics and the corresponding optical, thermal and electrical properties of the nanocomposite films.

2. Experimental section

2.1. Materials

Palladium chloride ($PdCl_2$), conc. hydrochloric acid (HCl) and dichloromethane (CH_2Cl_2) were purchased from Merck, India. Sodium borohydride ($NaBH_4$) and dodecanethiol ($C_{12}H_{25}SH$) were purchased from Aldrich, USA. Polycarbonate (Caliber T303, (M_w: 160,000)) was obtained from Dow Chemicals, USA. Deionized water with a resistivity of 18×10^4 Ωm was obtained from a Millipore unit.

2.2. Synthesis of Pd/PC nanocomposite films

In the *ex situ* method, $C_{12}H_{25}SH$-protected Pd nanoclusters were prepared using Brust method [24]. The Pd nanoclusters were then homogenously mixed with a solution of 40 mg of PC in 20 ml of CH_2Cl_2 (1.6 μM) followed by film casting at room temperature. In the case of the *in situ* method, PC (40 mg) was dissolved in CH_2Cl_2 (20 ml) (1.6 μM). $PdCl_2$ (15 mg) was first dissolved in 2 ml of conc. HCl so as to form a complex $[PdCl_4]^{2-}$ and was further dissolved in 48 ml water to form a 1 mM solution. This biphasic mixture was stirred continuously using a magnetic stirrer for 30 min. A freshly prepared solution of $NaBH_4$ in 20 ml water (0.1 M) was added dropwise to the mixture. The color of the reaction mixture changed rapidly from golden yellow to black, indicating the formation of Pd nanoclusters. After stirring for 3 h, the organic phase was separated, washed with water and was directly cast into film at room temperature. Soon after the reduction nearly all of the reduced Pd nanoparticles get themselves shifted from aqueous phase to organic phase. Both the *ex situ* and *in situ* films were cast in two different thicknesses (20 μm and 3 μm). Films of 3 μm thickness were used for optical properties measurement as the 20 μm thick films were found to be nearly opaque. The remaining characterization methods involved the 20 μm thick films.

2.3. Characterization of Pd/PC nanocomposite films

TEM micrographs were taken on a JEOL model 1200 EX instrument operated at an accelerating voltage of 120 kV. Samples for TEM analysis were of a stock solution of 0.5 ml of 1 wt% nanocomposite solution in dichloromethane. These stock solutions were cast on a carbon coated Cu grid (400 meshes) and dried slowly at room temperature. FTIR spectroscopic measurements of the nanocomposite films were carried out on a Perkin–Elmer FTIR 1760 X spectrometer operating at a resolution of 4 cm^{-1} in the range of 300–4000 cm^{-1}. UV–vis spectra of samples were taken with an Ocean Optics USB 2000 spectrometer with an operating range from 300 nm to 1000 nm. Thermogravimetric analysis was performed using Perkin–Elmer TGA-7 thermal analysis system, operated under nitrogen flow in the temperature range of 50–700 °C with a heating rate of 20 °C/min. The calorimetric measurements were carried out using a DSC-7 (Pyris 1, Perkin–Elmer) unit over a temperature range of 20–200 °C. The samples were heated at the rate of 20 °C/min under nitrogen atmosphere. Electrical conductivity measurements were made on the nanocomposite films by using Keithley-237 source measure unit. The voltage was applied and the current flow was monitored. The leads (alligator clips) were directly clipped on the sample suspended in air. The experiment was repeated at several distances between the leads.

3. Results and discussion

3.1. Morphology of Pd/PC nanocomposites

The TEM image of the *ex situ* nanocomposite with 2 vol.% Pd (on a stoichiometric basis) revealed dispersed Pd nanoclusters of ~15(±0.6) nm embedded in PC matrix (Fig. 1a). Based on earlier reports on the synthesis and morphology of *n*-alkanethiol-protected Pd nanoclusters [15,20], the presence of dodecanethiol on the surface of the Pd nanoclusters in the present study is likely to ensure the separation of the nanoclusters even after mixing with PC. However, the average particle size of the Pd nanoclusters in

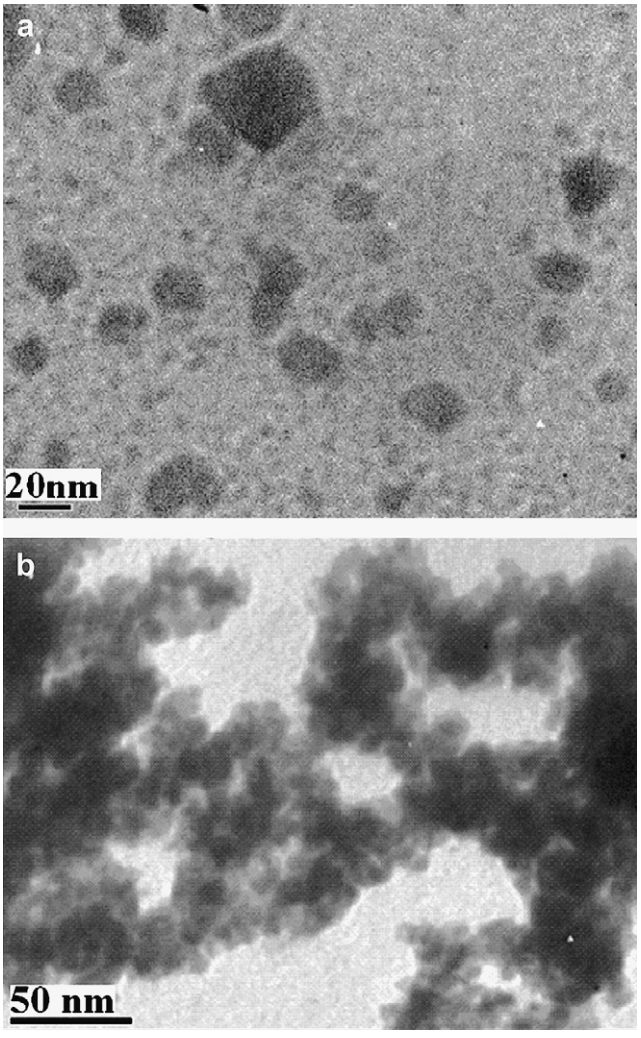

Fig. 1. TEM image of the *ex situ* and *in situ* Pd/PC nanocomposites showing (a) dispersed Pd nanoclusters, and (b) agglomerated Pd nanoclusters, respectively.

previous studies was found to be ~5 nm in size; using the Brust method [24]. Although the identical metal salt:thiol ratio and reducing agent were used in the present study, an increase in the size of the nanoclusters was found. This was confirmed to be at least partly due to the absence of the surfactant, tetraoctyl ammonium bromide, in the reaction mixture which helps in phase transfer of reduced Pd nanoclusters. The effect of increased temperature of the reaction mixture from ice-cold condition in the earlier studies in comparison to the reaction at room temperature may have also contributed to the increased size of the nanoclusters [25]. A difference in the concentration of reducing agent may have also contributed to the increase in the average size of nanoclusters.

In contrast to the above system, *in situ* nanocomposite of Pd nanoclusters (2 vol.% on a stoichiometric basis) in PC showed significant agglomeration (Fig. 1b). Similar observations on agglomeration were reported by Chen et al. using Pd/ mercapto-poly(ethylene glycol) [13], Chatterjee and Jewrajka with Au/ poly(dimethylamino ethyl methacrylate-*b*-methyl methacrylate) copolymers (mol. wt. 50,000) [21], and Coiberre et al. using Au/thiol terminated polystyrene (mol. wt. 80,000) [22]. However, discrete nanoclusters were also noted by Tamilselvan et al. in Au/poly (styrene-*b*-vinyl pyrrolidone) copolymer systems (mol. wt. 30,000, nanocluster size: ~9 nm) [26], and Khanna et al. [27] in Ag/ poly(vinyl alcohol) systems (mol. wt. 125,000, nanocluster size: ~10 nm). Thus, morphological changes in nanocomposites appear to be strongly dependent on the specific polymer system and reaction conditions.

Wang et al. have suggested that in order to obtain discrete nanoclusters, the rate of adsorption of organic ligands on the surface of nanoclusters should equal the rate of nanocluster formation [18]. Accordingly, organic ligands with lower molecular weight have generally been found to be more effective in limiting the nanoclusters' size [15,28]. The wide-ranging behavior of agglomeration in nanocomposites prepared by the *in situ* methods may also be due to the differences in the conformations of the polymer chain in different studies. These conformational differences can arise from variations in molecular weight, solvent, and temperature. Consequently, the mobility of the polymer during adsorption on the nanocluster surface can be affected, thereby limiting the agglomeration of the nanoclusters. In addition, the nature of interactions between the polymer and the surface of the nanoclusters may also play a role in determining the morphology of the resulting nanocomposites. Further studies are needed to better understand the differences in morphologies observed between the *in situ* and *ex situ* nanocomposites. The following sections examine the consequences of the differences in morphology on the resulting properties of the nanocomposites.

3.2. Chemical interactions of Pd/PC nanocomposites

The FTIR spectra for PC, the *ex situ* and *in situ* Pd/PC nanocomposites are shown in the Fig. 2. All peak positions of PC and the nanocomposites were assigned and tabulated in Table 1 along with references from prior studies [29–37]. From the figure, we can confirm that at high wavenumber region (2600–3200 cm^{-1}), no major differences can be noted between PC and the *in situ* nanocomposite. However, with the *ex situ* nanocomposite two new peaks at 2922 cm^{-1} and 2851 cm^{-1} were seen. From the assignments, it can be concluded that the appearance of these peaks is due to the presence of alkyl chains from dodecanethiol adsorbed on Pd nanoclusters in the *ex situ* nanocomposite.

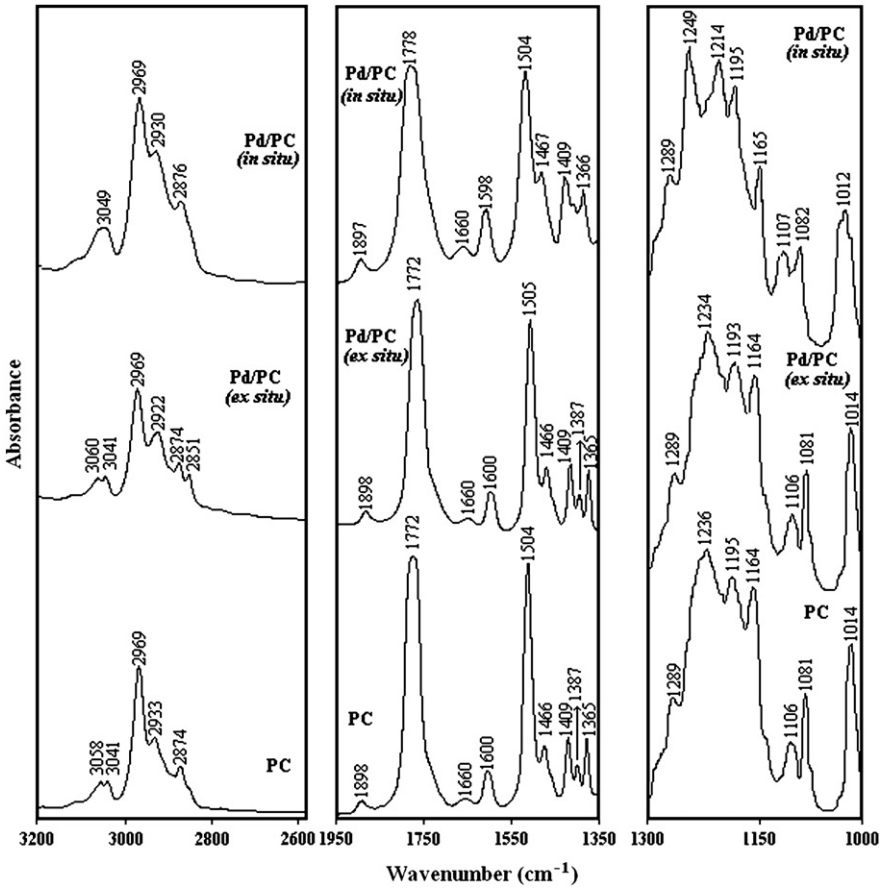

Fig. 2. FTIR spectra of PC and the *in situ* and *ex situ* Pd/PC nanocomposites.

Table 1
FTIR peaks for PC and Pd/PC nanocomposites

PC	Pd/PC (*ex situ*)	Pd/PC (*in situ*)	Description for the bands observed	Ref.
3058	3060	–	C–H stretching for phenyl	[29]
–	–	3049	C–H stretching for phenyl	
3041	3041	–	C–H stretching for phenyl	
2969	2969	2969	C–H asymmetric stretching for $-CH_3$	[30]
2933	–	2930	C–H symmetric stretching for CH_3 (Fermi)	
–	2922	–	C–H asymmetric stretching for CH_2	
2874	2874	2876	C–H symmetric stretching for CH_3	
–	2851	–	C–H symmetric stretching for CH_2	
1772	1772	1778	C═O stretching vibration (1785 cm^{-1} *cis–trans*; 1767 cm^{-1} *trans–trans*)	[31,37]
1660	1660	1660	C═C stretching for phenyl	
1600	1600	1598	C–C in-plane stretching for phenyl (1604 cm^{-1} *cis–trans*; 1594 cm^{-1} *trans–trans*)	
1504	1505	1504	C–C in-plane stretching for phenyl	[32–34]
1409	1409	1409	C–C symmetric in-plane stretching for phenyl	[32,33]
1387	1387	–	C–H asymmetric bending vibration of CH_3	[35]
1365	1365	1366	C–H symmetric bending vibration of CH_3	
–	–	1249	C–O–C asymmetric stretching (*trans–trans*)	[31]
1236	1234	–	C–O–C asymmetric stretching	
–	–	1214	C–O–C asymmetric stretching (*cis–trans*)	
1195	1193	1195	C–O–H stretching	[29]
1165	1164	1164	C–O–C symmetric stretching	
1106	1106	1107	C–H in plane bending for *o,p*-substituted benzenes	
1081	1081	1082	C–C–C bend for phenyl	
1014	1014	1012	C–C–C in plane bend C–O stretching for aryl–O–C	[31,33,36]

In the wavenumber region of 1350–1950 cm^{-1}, the peak trends of the PC and the *ex situ* nanocomposites were nearly the same. However, the –C═O peak showed a red shift to 1778 cm^{-1} for the *in situ* nanocomposites. The shift was also accompanied with a broadening of peak from 39 cm^{-1} to 64 cm^{-1} (bandwidth at half maximum is shown in Table 2). This may have arisen due to the conformational changes in the PC as noticed by Heymans and Rossum [31] and Dybal et al. [37] or due to chemical interactions between the carbonyl group of PC and the Pd nanoclusters. Additionally, a minor change in the peak position at 1598 cm^{-1} was noted for the *in situ* nanocomposite. Similar to prior explanations by Heymans and Rossum [31] this may be due to conformational changes in the phenyl ring of the PC.

Two new peaks at 1249 cm^{-1} and 1214 cm^{-1} were noticed for the *in situ* nanocomposite instead of the 1236 cm^{-1} peak that can be noticed in PC and the *ex situ* nanocomposite. From the assignments in Table 1, we can infer that there is a possibility of conformational changes in the –C–O–C– group of the PC chains when they interact directly with Pd nanoclusters. Other changes that can be observed in the low wavenumber region include the reduction in the peak intensities at 1164 cm^{-1}, 1082 cm^{-1} and broadening of peak at 1012 cm^{-1} for the *in situ* nanocomposites, usually associated with the C–O–C symmetric stretch, phenyl bending and aromatic C–O stretching, respectively.

Taken together, it may be concluded that the proximity to the Pd nanocluster surface can induce significant conformational changes in the PC chains in the *in situ* nanocomposite. However, the presence of the dodecanethiol monolayer appears to prevent such perturbations in the *ex situ* nanocomposite. Further research is required to sufficiently explain the changes in the polymer vibrational modes since the possibility of complicating factors such as scattering effects and electromagnetic field changes due to the presence of the metal nanoclusters cannot be ruled out.

Table 2
The bandwidth at half maximum for various peaks in PC and the *in situ* and *ex situ* Pd/PC nanocomposites

Sample	Peak position (cm^{-1})	Bandwidth at half maximum (cm^{-1})
PC	1772	39
Pd/PC (*ex situ*)	1772	42
Pd/PC (*in situ*)	1778	64
PC	1012	16
Pd/PC (*ex situ*)	1012	16
Pd/PC (*in situ*)	1014	26

3.3. Optical properties

Transmittance spectra of the 3 μm thick *ex situ* and *in situ* Pd/PC nanocomposite films (2 vol.% Pd on a stoichiometric basis) in the UV–vis–IR region (400–1000 nm) are shown in Fig. 3. It can be observed that the transmittance of the *ex situ* nanocomposite film was higher than that observed for the *in situ* nanocomposite film at any wavelength in the investigated UV–vis–IR region. However, similar to the prior work by Checchetto et al. [38], the percentage transmittance of light by PC remains nearly constant at 70 (±0.2)% from 400 nm through 800 nm. Early reports studied the influences of concentration, size, shape, and size distribution of the nanoparticles as well as the molecular weight of the protecting agent on the optical properties of the nanocomposites. For example, Aymonier et al. [11] with Pd/PMMA, Akamatsu et al. [39] with Ag/Nylon, and Nemamcha et al. [40] with Pd/poly(vinyl pyrrolidone) have shown that the transmittance of light in the UV–vis region decreased with increase in the metal nanoparticle concentration. Chang et al. [41] on their work on Au nanorods stated that the absorption peaks shift towards red as the mean aspect ratio of the particle increases. Balamurugan and Maruyama [42] noted a red shift in the peak positions with the increase in the particle size. The work of Jiang et al. [43] on the synthesis of Au nanorods explains the influence of shapes like cube, sphere and unshaped particles on the absorption spectra of Au nanoparticles. Gao et al. [44] found that the plasmon absorption maxima (inversely proportional to transmittance) of Au nanoparticles decrease with increase in the size of the capping agent, alkyltrimethylammonium bromide. Gole and Murphy [45] found that in the case of Au nanorods coated with polyelectrolyte, the plasmon absorption maxima of Au decrease with increase in the thickness of the coating. In complement to the above-mentioned reports, in our work, we tried to study the influence of nanocomposite film morphology on the transmittance of light in the UV–vis–IR region. Further studies are required for understanding the optical properties of these nanocomposites in a detailed manner.

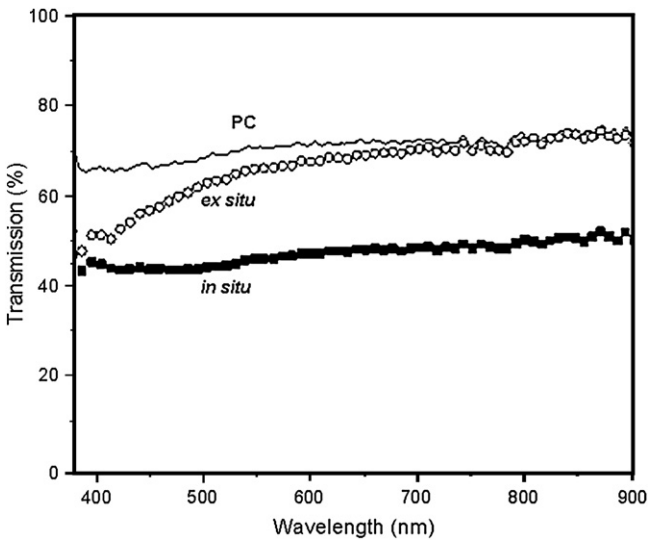

Fig. 3. Comparison of transmission spectra of 3 μm thick PC and the *in situ* and *ex situ* Pd/PC nanocomposite films with 2 vol.% Pd content.

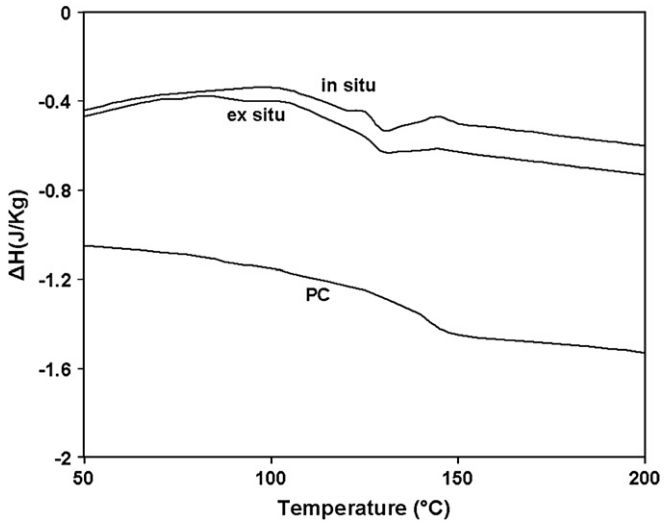

Fig. 4. DSC measurements showing reduction in the T_g of the *in situ* and *ex situ* Pd/PC nanocomposites when compared to free PC.

3.4. Thermal properties

A comparison of the DSC profiles of the nanocomposites is shown in Fig. 4. It was found that the T_g of both the *ex situ* and *in situ* nanocomposites (with 2 vol.% Pd on a stoichiometric basis) decreased by 16 °C (from 146(±2) °C to 130(±1) °C). Aymonier et al. [11] observed ~9 °C decrease in T_g for Pd/PMMA (Pd content: 0.01 vol.%) nanocomposites synthesized by a different route. Differences in concentration (≤0.1 wt%) and nanocluster size (~2 nm) between their work and the present study may account for differences in the magnitude of the change in T_g. Earlier studies by Liu et al. [13] using Au/PMMA (molar ratio: 1:5.25) and Hsu et al. [46] with Au/polyurethane (Au content: 0.065 wt%) also showed a decrease in T_g by 20 °C and 5 °C, respectively. Prior studies with fumed silica-based poly(4-methyl-2-pentyne) and poly(1-trimethylsilyl-1-propyne) nanocomposites indicated a substantial rise in gas permeability compared to the unfilled polymers suggesting an increase in free volume between the polymer chains [47,48]. In a similar manner, the Pd nanoclusters embedded may have increased the free volume between the PC chains, thereby reducing the T_g of the nanocomposites. However, an increase in T_g by 7 °C was also noted by Ash et al. [49] in alumina/PMMA nanocomposites

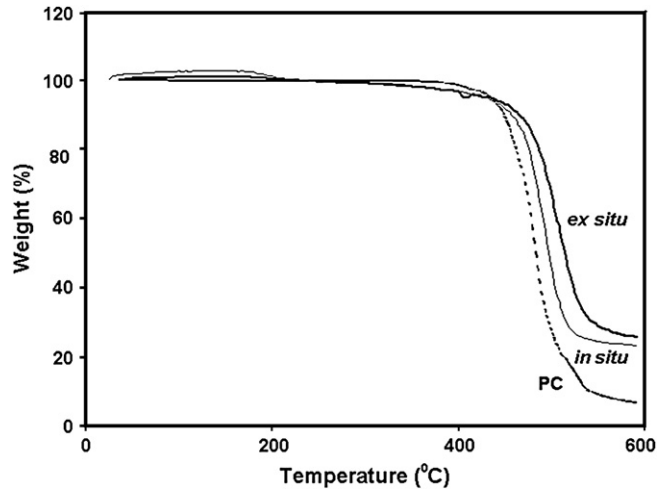

Fig. 5. Thermogravimetric analysis of the *in situ* and *ex situ* Pd/PC nanocomposites show increased thermal stability when compared to the unfilled PC.

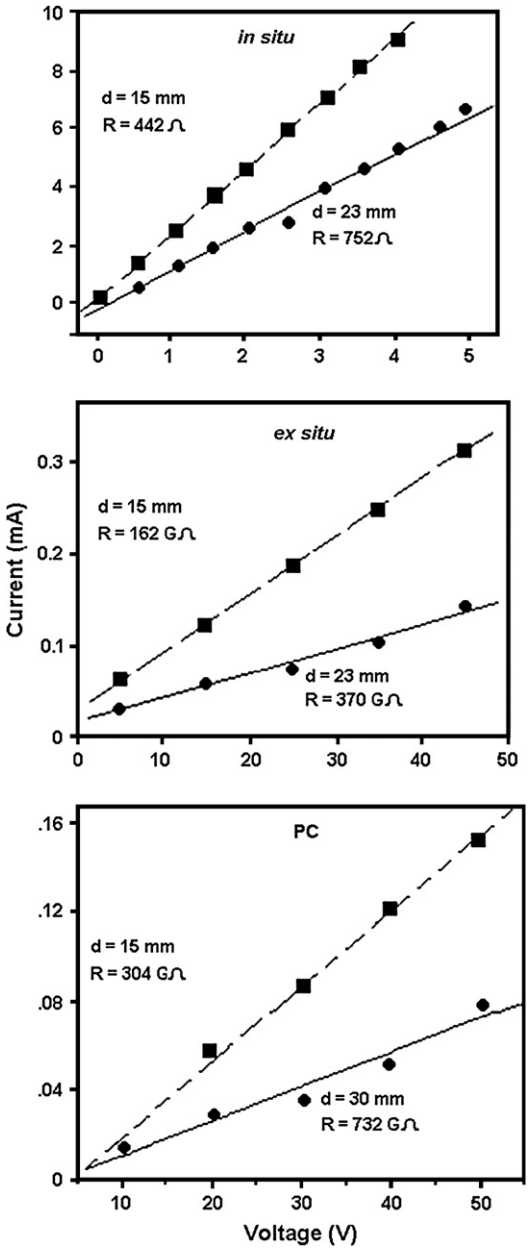

Fig. 6. *I–V* measurements of *in situ* (resistivity = 2.1×10^5 Ωm) and *ex situ* Pd/PC nanocomposites (resistivity = 7.2×10^{13} Ωm) along with unfilled PC (resistivity = 2.1×10^{14} Ωm). [*Note*: d = distance between the electrodes and R = resistance.]

(Alumina content: 10 wt%). The presence of strong interactions between the carbonyl groups of PMMA and alumina is well known [50]. Consequently, the polymer chains will be strongly pinned to the surface of the metal oxide, thereby increasing T_g. In contrast, relatively weak interactions exist in the Pd/PC nanocomposites as evidenced by the FTIR data. Similarly, relatively weak interactions between the filler and polymer are likely to exist in the fumed silica and Au-based nanocomposites, resulting in an increase in free volume and a corresponding decrease in T_g.

Thermogravimetric analysis performed under nitrogen (Fig. 5) indicated that the incorporation of Pd nanoclusters in PC for the *ex situ* nanocomposite increased the thermal stability of the PC matrix from ~430(±5) °C to ~470(±2) °C. In comparison, in the *in situ* nanocomposite an improvement in thermal stability to ~450(±2) °C was observed. A similar rise in thermal stability was noted in earlier reports by Huang et al. [51] for Au/poly(methyl styrene) (particle size: 3.5 nm and Au content: 5 wt%), Aymonier

et al. [11] for Pd/PMMA (particle size: 2.5 nm) and Hsu et al. [46] for Au/polyurethane (particle size: 5 nm). Aymonier et al. [11] and Hsu et al. [46] also observed that the thermal stability of the nanocomposites increases with increase in metal concentration and with decrease in particle size and agglomeration. These results are based on changes in area of the polymer–nanocluster interface and are in close agreement with the present study.

3.5. Electrical conductivity

The influence of Pd nanoclusters on the electrical behavior of 20 μm thick Pd/PC nanocomposite films is shown in Fig. 6. PC is electrically insulating in nature with a volume resistivity of about $2.1(\pm0.1)\times10^{14}\,\Omega$m. No significant difference is observed for the *ex situ* nanocomposite which showed a resistivity of $7.2(\pm0.2)\times10^{13}\,\Omega$m. However, the *in situ* nanocomposite showed a linear increase in the current with the voltage indicating a constant resistance of about $442(\pm19)\,\Omega$ and thus a resistivity of $2.1(\pm0.1)\times10^{5}\,\Omega$m. Similar results were seen in earlier studies by Athawale et al. [52] on Pd/polyaniline nanocomposites and Rao and Trivedi [53] on Pd/polypyrrole nanocomposites. However, these studies involved conducting polymers in contrast to an electrically insulating polymer (PC) in the present work. The origin of the striking differences in the behavior of the *in situ* and *ex situ* nanocomposites is not completely clear. The insulating nature of the *ex situ* nanocomposite appears reasonable because of the presence of discrete Pd nanoclusters. Here, the nanoclusters would be separated from each other by dodecanethiol before being embedded into the PC matrix. However, the *in situ* nanocomposite, the agglomerated Pd nanoclusters also appear to be discrete islands of agglomerates in the polymer. Further work is therefore necessary to understand the differences in electrical conductivity in the *in situ* and *ex situ* nanocomposites.

4. Conclusions

Pd/PC nanocomposites prepared by the *ex situ* and *in situ* methods exhibited marked differences in their morphology. The Pd nanoclusters produced by the *ex situ* method were well dispersed while the Pd nanoclusters produced by the *in situ* method were agglomerated. In the absence of any capping agent such as thiol or polymer, stable Pd nanoclusters could not be obtained due to inadequate stabilization. FTIR data of the PC and the *in situ* and *ex situ* nanocomposites showed significant changes in the peak positions *in situ* nanocomposites, suggesting possible conformational changes in the PC chains in the presence of the Pd nanoclusters. The nanocomposites exhibited a strong dependence of optical, thermal and electrical properties on their morphology. For the same Pd content, the *ex situ* nanocomposites were found to transmit more light than the *in situ* nanocomposites in the UV–vis–IR region. The T_g of both the nanocomposites was lower than PC by 16 °C. In addition, the onset of thermal degradation of the *ex situ* and *in situ* nanocomposites was found higher than PC by 40 °C and 20 °C, respectively. The electrical properties of these nanocomposites suggest that the *in situ* method is best suited to make electrically conducting metal–polymer nanocomposites. Taken together, it can be concluded that the two synthesis procedures have a pronounced influence on the morphology and properties of Pd/PC nanocomposites.

References

[1] Ziolo RF, Giannelis EP, Weinstein BA, O'Horo MP, Ganguly BN, Mehrotra V, et al. Science 1992;257:219–23.
[2] Wuelfing WP, Gross SM, Miles DT, Murray RW. Journal of the American Chemical Society 1998;120:12696–7.
[3] Aslam M, Mulla IS, Vijayamohanan K. Langmuir 2001;17:7487–93.
[4] Aslam M, Mulla IS, Vijayamohanan K. Applied Physics Letters 2001;79:689–91.
[5] Aslam M, Gopakumar G, Shoba TL, Mulla IS, Vijayamohanan K, Kulkarni SK, et al. Journal of Colloid and Interface Science 2002;255:79–90.
[6] Liu FK, Hsieh SY, Ko FH, Chu TC, Dai BT. Japanese Journal of Applied Physics, Part 1: Regular Papers and Short Notes and Review Papers 2003;42:4147–51.
[7] Whetten RL, Khoury JT, Alvarez NM, Murthy S, Vezmar I, Wang ZL, et al. Advanced Materials 1996;8:428–33.
[8] Gonsalves KE, Carlson G, Chen X, Gayen SK, Perez R, Yacaman MJ. Nanostructured Materials 1996;7:293–303.
[9] Huang H, Yuan Q, Yang X. Colloids and Surfaces B: Biointerfaces 2004;39:31–7.
[10] Chattopadhyay S, Datta A. Synthetic Metals 2005;155:365–7.
[11] Aymonier C, Bortzmeyer D, Thomann R, Mulhaupt R. Chemistry of Materials 2003;15(25):4874–8.
[12] Houdayer A, Schneider R, Billaud D, Ghanbaja J, Lambert J. Applied Organometallic Chemistry 2005;19:1239–48.
[13] Liu FK, Hsieh SY, Ko FH, Chu TC. Colloids and Surfaces A: Physicochemical and Engineering Aspects 2002;231(1–3):31–8.
[14] Sondi I, Goia DV, Matijevc E. Journal of Colloid and Interface Science 2003;260:75–81.
[15] Zamborini FP, Gross SM, Murray RW. Langmuir 2001;17:481–8.
[16] Henglein A, Giersig M. Journal of Physical Chemistry B 1999;103:9533–9.
[17] Ramirez E, Jansat S, Philippot K, Lecante P, Gomez M, Bulto AMM, et al. Journal of Organometallic Chemistry 2004;689:4601–10.
[18] Wang H, Qiao X, Chen J, Ding S. Colloids and Surfaces A: Physicochemical and Engineering Aspects 2005;256:111–5.
[19] Chen M, Falkner J, Guo WH, Zhang JY, Sayes C, Colvin VL. Journal of Colloid and Interface Science 2005;287:146–51.
[20] Sun Y, Frenkel AI, Isseroff R, Shonbrun C, Forman M, Shin K, et al. Langmuir 2006;22:807–16.
[21] Jewrajka SK, Chatterjee U. Journal of Polymer Science Part A: Polymer Chemistry 2006;44(6):1841–54.
[22] Corbierre MK, Cameron NS, Sutton M, Laaziri K, Lennox RB. Langmuir 2005;21:6063–72.
[23] Rong M, Zhang M, Liu H, Zeng H. Polymer 1999;40:6169–78.
[24] Walker BM, Bethell M, Schiffrin D, Whyman DJ. Journal of the Chemical Society and Chemical Communications 1994;20:801–2.
[25] Koga K, Ikeshoji T, Sugawara K. Physical Review Letters 2004;92:11507-1–11507-4.
[26] Tamilselvan S, Hayakawa T, Nogami M, Kobayashi Y, Marzan L, Hamanaka Y, et al. Journal of Physical Chemistry 2002;106:10157–62.
[27] Khanna PK, Singh N, Charan S, Subbarao VVVS, Gokhale R, Mulik UP. Materials Chemistry and Physics 2005;93:117–21.
[28] Yukihide S, Naoki T. Colloids and Surfaces A: Physicochemical and Engineering Aspects 2000;169:59–66.
[29] Wang J, Montville D, Gonsalves KE. Journal of Applied Polymer Science 1999;72:1851–68.
[30] Laibinis PE, Whitesides GM, Allara DL, Tao YT, Parikh AN, Nuzzo RG. Journal of the American Chemical Society 1991;113:1128–32.
[31] Heymans N, Rossum SV. Journal of Materials Science 2002;37:4273–7.
[32] Hopfe I, Pompe G, Eichhorn KJ. Polymer 1997;38(10):2321–7.
[33] Ning P, Ko TM. Polymer Engineering and Science 1997;37(7):1226–37.
[34] Liu CK, Hu CT, Lee S. Polymer Engineering and Science 2005;45(5):687–93.
[35] Dehaye F, Balanzat E, Ferain E, Legras R. Nuclear Instruments and Methods in Physics Research B 2003;209:103–12.
[36] Wang Y, Jin Y, Zhu Z, Liu C, Sun Y, Wang Z, et al. Nuclear Instruments and Methods in Physics Research B 2000;164:420–4.
[37] Dybal J, Schimdt P, Baldrian J, Kratochvil J. Macromolecules 1998;31:6611–8.
[38] Checchetto R, Miotello A, Chayahara A. Journal of Physics: Condensed Matter 2000;12:9215–20.
[39] Akamatsu K, Takei S, Mizuhata M, Kajinami A, Deki S, Takeoka S, et al. Thin Film Solids 2000;359:55–60.
[40] Nemamcha A, Rehsrpringer JL, Khatmi D. Journal of Physical Chemistry B 2006;110:383–7.
[41] Chang SS, Shih CW, Chen CD, Lai WC, Wang CRC. Langmuir 1999;15:701–9.
[42] Balamurugan B, Maruyama T. Applied Physics Letters 2005;87:143105–7.
[43] Jiang XC, Brioude A, Pileni M. Colloids and Surfaces A: Physicochemical and Engineering Aspects 2006;277:201–6.
[44] Gao J, Bender CM, Murphy CJ. Langmuir 2003;19:9065–70.
[45] Gole A, Murphy CJ. Chemistry of Materials 2005;17(6):1325–30.
[46] Hsu SH, Chou CW, Tseng SM. Macromolecular Materials and Engineering 2004;289:1096–101.
[47] Merkel TC, He Z, Pinnau I. Macromolecules 2003;36:6844–55.
[48] Ash BJ, Schadler LS, Siegel RW. Journal of Polymer Science, Part B: Polymer Physics 2004;42:4371–83.
[49] Ash BJ, Schadler LS, Siegel RW. Materials Letters 2002;55:83–7.
[50] Tirrell M, Tannenbaum R, King S, Lecy J, Potts L. Langmuir 2004;20:4507–14.
[51] Huang HM, Chang CY, Liu IC, Tsai HC, Lai MK, Tsiang CCR. Journal of Polymer Science, Part A: Polymer Chemistry 2005;43:4710–20.
[52] Athawale AA, Bhagwat SV, Katre PP. Sensors and Actuators B 2006;114:263–7.
[53] Rao CRK, Trivedi DC. Catalysis Communications 2006;7:662–8.